Co-expression of IL-7 and PH20 Promote anti-GPC3 CAR-T Tumor Suppressor Activity in Vivo and in Vitro

Qian Liu
Department of Clinical Laboratory, Hospital of Chengdu University of Traditional Chinese Medicine
Cixiao Wang
Nephrology Department II, Hospital of Chengdu University of Traditional Chinese Medicine
Zeyou Jiang
Department of Clinical Laboratory, Hospital of Chengdu University of Traditional Chinese Medicine
Su-yang Yue (suyangyue_1@163.com)
The Affiliated Huai'an Hospital of Xuzhou Medical University

Research

Keywords: hematological malignancies, CAR-T, tumors, hyaluronidase, vivo, vitro

Posted Date: August 5th, 2020

DOI: https://doi.org/10.21203/rs.3.rs-51247/v1

Abstract

While CAR-T therapy has successfully treated hematological malignancies, it has proved sub-optimal for solid tumors. The main limitation is the inability of CAR-T cells to infiltrate and then proliferate within tumors. In this study, we co-expressed IL-7 and PH20, a type of hyaluronidase, with CAR targeting GPC3 (G3CAR-7×20) to address these issues. We found (G3CAR-7×20) exhibited better proliferation *in vivo* and *in vitro* than G3CAR, reduced the level of apoptosis after stimulation by tumor cells, and maintained the memory phenotype of CAR-T cells. G3CAR-7×20 also increased the ability of CAR-T cells to infiltrate tumor tissue. G3CAR-7×20 may significantly enhance the efficacy of CAR-T cells in solid tumors.

Introduction

CAR-T cell therapy has demonstrated encouraging therapeutic effects when treating hematological malignancies [1, 2]. Two CAR-T treatments targeting CD19 have been launched successfully [3, 4]. CAR-T targeting the B-cell maturation antigen (BCMA) has also shown positive therapeutic effects in clinical trials[5–7]. However, CAR-T cell therapy has not yet had similar results in solid tumors[8–10]. Solid tumors have a more complex immunosuppressive microenvironment and there are many immunosuppressive cells and cytokines which inhibit the activation and survival of CAR-T cells within the tumor [11, 12]. The dense extracellular matrix (ECM) also prevents CAR-T cells from infiltrating into solid tumors and can affect CAR-T cell activity [13, 14].

During cultivation, additional cytokines, such as IL7 and IL15, can promote the effective proliferation and maintenance of the memory phenotype of CAR-T cells[15, 16]. However, adding extra IL-7 during cultivation has no effect *in vivo*. It is difficult for T cells, including CAR-T cells, to penetrate the extracellular matrix and thus infiltrate the tumor [13, 14]. Reports suggest that recombinant hyaluronidase rHPH20 has a greater clinical effect on ECM degradation, promoting lymphocyte infiltration into tumor cells[17, 18]. PH20 is a GPI-anchored membrane protein which may play a positive role in CAR-T cell treatment of solid tumors [19].

Hepatocellular carcinoma (HCC) is a highly aggressive and fast-growing malignancy with high lethality which lacks effective treatment [20, 21]. There are many clinical trials of CAR-T cell therapy for HCC [22]. However, treatment efficacy to date has not proved satisfactory. The immunosuppressive microenvironment and the ECM in particular trouble CAR-T HCC treatment[23]. In this study, we used CAR-T targeting GPC3 and co-expressed IL-7 and PH20 (G3CAR-7 × 20) as a putative treatment for HCC. Compared to traditional GPC3 targeted CAR-T, G3CAR-7 × 20 showed improved infiltration and expansion in tumor tissue. Tumor suppression speed was faster, and resistance to relapse was greater. This research should provide the basis for a fruitful new strategy in HCC treatment.

Results

Design and characterization of G3CAR-7×20

The structure of G3CAR-7×20 is shown in figure 1A. We created a tandem construct encoding CAR, IL-7, and PH20 with two 2A peptide sequence linking the genes and cloned this into a lentivirus vector. A vector expressing CAR (G3CAR) only was used as a control. After transduction, all constructs were expressed stably by human peripheral blood T cells (Figure 1B). Compared to C3CAR, the G3CAR-7×20 construct had slightly lower transduction efficiency. This may be due to the larger ORF of G3CAR-7×20. To test IL-7 production, we took supernatants from Non-transduction T cell (NT-T) or G3CAR or G3CAR-7×20, co-cultured with or without GPC3+ tumor cells Huh7, and measured IL-7 using ELISA. As shown in Figure 1C, compared to G3CAR or NT-T, IL-7 secretion by G3CAR-7×20 is significantly increased, irrespective of tumor cell activation. 10 days post transduction, PH20 expression was measured by Western blot, as shown in Figure 1D. PH20 expression by G3CAR-7×20 was significantly higher than by G3CAR or NT-T.

Overexpressed IL-7 promotes CAR-T proliferation and maintains memory phenotype

During the culture of CAR-T cells *ex vivo*, we found G3CAR-7×20 proliferated faster than G3CAR (Figure 2A). We hypothesized that overexpression of IL-7 promotes the proliferation of CAR-T cells. Therefore, we tested the proliferation rate of G3CAR (with and without IL-7 supplementation) and G3CAR-7×20 *ex vivo*. As Figure 2B shows, the proliferation rate of G3CAR and NT-T increased significantly after addition of IL-7, then becoming similar to that of G3CAR-7×20.

Previous reports suggest IL-7 could maintain the memory phenotype of T cells. Thus we tested the phenotype of G3CAR-7×20 and G3CAR. Memory cells (naïve T, Tscm, and Tcm) are a CCR7+ population. We found G3CAR-7×20 had a significantly higher proportion of cells with the memory phenotype than did G3CAR. It is also of note that CAR negative T cells in the G3CAR-7×20 culture had a higher proportion of memory cells than G3CAR. That may be because secreted IL-7 can stimulate surrounding cells (Figure 2C). To substantiate this assertion, we generated a model, as shown in Figure 2D. Briefly, we collected the supernatant from G3CAR-7×20 and G3CAR each cultured for 24 hours without cytokine. We then added this supernatant to T cells electro-transfected with the STAT5 report vector. After 24 hours, fluorescence intensity was measured using the ONE-Glo® Luciferase Assay System. As shown in Figure 2E, the fluorescence intensity of G3CAR-7 × 20 supernatant is higher than that of G3CAR supernatant. This adds support to our conjecture that overexpression of IL-7 could act on surrounding cells and potentially play an important role in CAR-T cell proliferation and the maintenance of memory phenotypes.

Overexpressed PH20 could increase Cell invasion capacity

To investigate if overexpressed PH20 could enhance the ability of CAR-T to invade tumors, we used BioCoat™ Matrigel® Invasion Chambers. As shown in Figure 3A, G3CAR-7×20 had a greater ability to invade tumors than did G3CAR. To evaluate if this increased capacity depended on the enzymatic activity of PH20, we established a Hyaluronan Sythase 2 (HSA2) overexpressing Huh7 cell line (Huh7-HSA2),

which could synthesize hyaluronan. CAR-T cells (G3CAR-7×20 and G3CAR) were co-cultured with Huh7-HSA2 for 8 or 24 hours and the supernatant collected, to allow detection of hyaluronan using a Hyaluronan Quantikine ELISA Kit. As shown in Figure 3B, G3CAR-7×20+Huh7-HAS displayed lower levels of hyaluronan than did G3CAR+Huh7-HAS. This suggests that overexpressed PH20 could improve the tumor invasion propensities of CAR-T therapy.

Cytotoxicity against tumor cell of G3CAR-7×20 in vitro

We next explored if IL7 and PH20 overexpression altered CAR-T cytotoxicity against tumor cells. We choose 3 types of GPC3 positive HCC cell line: HepG2 , Huh7 and PLC/PRF/5. We first evaluated the short-term cytolysis capacity of G3CAR-7×20, G3CAR, and NT-T versus the three HCC cell lines. As shown in figure 4A, both G3CAR-7×20 and G3CAR, when tested with equivalent ET ratios, had a similar cytotoxicity against GPC3+ cell lines. However, the long-term cytotoxicity of G3CAR-7×20 was greater than G3CAR (Figure 4B). We suspect this greater cytotoxicity is caused by the enhanced capacity of G3CAR-7×20 to proliferate and inhibit apoptosis after activation. Thus, we labeled CAR-T cells with CFSE and co-cultured them with tumor cells at 1:5 ET ratio for 96 hours. As shown in Figure 4C-E, G3CAR-7×20 exhibited longer proliferation times and a higher rate of proliferation. We next monitored CAR-T apoptosis during tumor cell encounter using PI staining. As shown in Figure 4F

, G3CAR-7×20 had lower levels of apoptosis than did G3CAR. For secreted cytokines, there was no significant difference between G3CAR-7×20 and G3CAR after tumor cell stimulation (see Figure 5). That may be regarded as a good predictor of clinical safety.

Activity of G3CAR-7×20 in vivo

To explore CAR-T anti-tumor ability in vivo, we established Huh7-HSA2 xenografts in NSG mice. $3*10^6$ CAR-T cells were injected i.v. when the mean tumor volume exceeded $300mm^3$. As shown in Figure 6A, G3CAR-7×20 exhibited a more rapid tumor suppressive activity than did G3CAR. Moreover, after 24 days CAR-T infusion, 3 mice receiving G3CAR CAR-T cells had relapsed. At days 0, 7, 14, 28 and 58 after CAR-T infusion, 50ul peripheral blood was removed from the tail vein. IL-7 did not increase dramatically, which may be due to local IL-7 secretion within tumors. IFN-gamma was detected in both G3CAR and G3CAR-7×20 at equivalent levels (see Figure 6B). During early CAR-T treatment, CAR-T cells expanded vigorously; by the 14th day, more G3CAR-7×20 than G3CAR T cells were detected in peripheral blood (see Figure 6C).

Unsurprisingly, mice receiving G3CAR-7×20 had a longer survival time than those receiving G3CAR (see Figure 6D). Body weight is not affected by IL-7 and PH20 expression, which may partly explain the apparent safety of G3CAR-7×20 *in vivo* (Figure 6E). We created a re-challenge model to investigate the durability of G3CAR-7×20. Huh7-HSA2 cells were injected into the right flank of NSG mice. After 11 days, the mean tumor volume was approximately $180mm^3$. $3*10^6$ CAR-T cells were then infused by i.v.., with the tumor volume measured every 4 days. After 20 days, tumors were virtually eliminated. 2*106 Huh7-

HSA2 cells were also injected into the left flank of the mice, again with the tumor volume measured every 4 days. As shown in Figure 6F, the left tumor recurred in mice treated with G3CAR but not with G3CAR-7×20.

Next, we investigated if this treatment effect is related to greater infiltration and longer survival of G3CAR-7×20 treated mice. We created additional xenograft models. CAR-T cells were labelled with CFSE and infused via the tail vein. After 3 and 7 days CAR-T infusion, 3 mice in each group were euthanized. We analyzed human CD3 cell infiltration into tumor tissues by ImmunoHistoChemistry (IHC), measuring the fluorescence intensity of CFSE-labelled human CD3 cells using FACS analysis (see Figures 7A and B). Infiltration of CD3 T cells seen in G3CAR-7×20 treated mice was significantly greater than in G3CAR mice. Moreover, T cells in G3CAR-7×20 mice tended to divide and proliferate more often than in G3CAR mice. These results support the view that G3CAR-7×20 has a greater anti-tumor efficacy *in vivo*, mediated by its overexpression of IL-7 and PH20.

Materials And Methods

Cell culture

Tumor cells HepG2 (ATCC® HB-8065), PLC/PRF/5 (ATCC® CRL-8024) were obtained from ATCC. Huh7 cell lines were obtained from Antihela BioTech. 293T cell were obtained from TAKARA (Lenti-X™ 293T Cell Line, 632180). All cell lines were cultured using DMEM medium (Gibco, 10564011).

Lentivirus and CAR-T preparation

The G3CAR gene comprises GC33 scFv, CD8a hinge and transmembrane domain, and the signaling domains of 4-1BB and CD3zeta[24]. To echo the gene structure of G3CAR, sequences corresponding to IL-7 and PH20 gene were placed in tandem, downstream of G3CAR, linked by a 2A sequence to form G3CAR-7×20. Both G3CAR and G3CAR-7×20 were cloned into a lentivirus vector.

The lentivirus vector and two helper vectors were transduced into 293T cell for 48 hours. The supernatant was then collected and purified using a Lenti-X Concentrator (TAKARA, 631232). The lentivirus titer was measured using a Lenti-X™ p24 Rapid Titer Kit (TAKARA, 632200), following manufacturer's instructions.

To prepare CAR-T, PBMCs supplied by healthy donors were stimulated using CTS™ (Cell Therapy Systems) Dynabeads™ CD3/CD28 (thermofisher, 40203D), and cultured in T cell medium (X-VIVO 15 medium contained 5%FBS and 100IU/ml IL-2 (Peprotech, 200-02)). After 24 hours, lentivirus was added with MOI at 3. CAR-T cells were then cultured in T cell medium for 10 days.

Flow cytometry assay

To detect transduced CAR-T, CAR-T cells were labeled with Human Glypican 3 / GPC3 Protein, His Tag (ACRO, GP3-H52H4-1mg) for 30min. After washing with PBS, the cells were stained using APC anti-His Tag Antibody (biolegend, 362605).

For detection of memory phenotype, CAR-T cells were labeled with Human Glypican 3 / GPC3 Protein, His Tag, and then stained using APC anti-His Tag Antibody and PE anti-human CD197 (CCR7) Antibody (biolegend, 353203). The cells were analyzed using BD Conto II. Subsequent data analysis was performed using Flowjo V10.

Western blot

WB analysis was performed as previously described. The primary antibodies used were PH20 (Abcam, ab196596) and GAPDH (Abcam, ab9485).

Cytokines detection

$1*10^5$ T cells were co-cultured, with or without equal quantities of tumor cells, for 18 hours and the supernatant collected. IL-2 and IFN-gamma were quantified using Human, Th1/Th2, Cytokine Kit II (BD, 551809), following the manufacturer's instructions. IL-7 was quantified using a Human IL-7 Quantikine HS ELISA Kit (R&D HS750). For hyaluronic acid detection, CAR-T cells (G3CAR-7×20 and G3CAR) were co-cultured with Huh7 and Huh7-HSA2 respectively for 24 hours and the supernatant collected. Hyaluronan was detected using a Hyaluronan Quantikine ELISA Kit.

Cell proliferation

Cell counts were quantified using a Cellometer Auto 2000.

For the CFSE based assay, CAR-T cells were labeled using a CellTrace™ CFSE Cell Proliferation Kit (ThermoFisher C34554). Cells were co-cultured with or without tumor cells for 96 hours and detected using standard FACS, with analysis performed using Flowjo V10.1.

Cell invasion assay

Invasive capacity was assessed using Corning® BioCoat™ Matrigel® Invasion Chambers (Corning, 354480), following manufacturer's instructions. The lower chamber contained 10% FBS medium as chemoattactant. As a control, the same experimental method was performed using 8.0 μm PET Membrane without a matrigel coating. The invasion percentage was calculated thus: (mean of cells invading through the Matrigel chamber membrane/mean of cells migrating through the control insert membrane) × 100.

Cytotoxicity assay

The CAR-T cells were co-cultured with tumor cells in round bottom 96-well-plates at different ET ratios for 4 hours or 24 hours, as required. The supernatant was collected and analyzed using a CytoTox 96® Non-Radioactive Cytotoxicity Assay (Promega, G1780), following manufacturer's instructions. The percentage of lysis was calculated as follows: [(experimental - spontaneous release) / (maximum load - spontaneous release) * 100(%)].

STAT5 report assay

CD3+ T cells, sorted using a Dynabeads™ FlowComp™ Human CD3 Kit (ThermoFisher 11365D), were electro-transfected with pGL4.52 [luc2P/STAT5 RE/Hygro] Vector (Promega E465A). CAR-T cells were simultaneously cultured without any cytokines. After 24 hours, the culture medium of the T cells transfected with a STAT report vector was replaced by that of the CAR-T cells. Cell culture continued for an additional 24 hours. Cells (50ul contains $1*10^5$ cells) were then transferred into a black assay plate and supplemented with 50 μL of Dual-Luciferase® Reporter Media before incubation for 20min. Fluorescence was then measured using an Envision Multilabel Reader (PerkinElmer).

Xenogenic mouse models

6-8 week-old male NSG mice (Jackson Laboratory) were injected subcutaneously with $2.5*10^6$ Huh-7-HSA2 cells. The tumor volume was measured every 4 days using a Vernier caliper (V= ½ x L (length) x W (width) x W). CAR-T cells were injected intravenously when the tumor volume exceeded $300mm^3$. Body mass was measured every 4 days.

Blood was collected from the tail vein. After centrifugation, plasma was collected for cytokine detection using BD™ CBA Flex Set (558334 and 561515). Cells were treated with Red Blood Cell Lysis Buffer (Beyotime, Shanghai, China) and stained using APC Mouse Anti-Human CD3ε (BD, 558257). T cells were counted and analyzed using CountBright™ Absolute Counting Beads.

For the tumor re-challenge model, $2*10^6$ CAR-T cells were injected intravenously when the mean tumor volume in the right flank exceeded $180mm^3$. $2*10^6$ Huh7-HSA2 was injected subcutaneously into the left flank. The tumor volume was measured every 4 days.

Immunohistochemistry (IHC)

For the IHC assay, tumor tissue samples were fixed, processed, and stained according to standard IHC procedures, as previously reported[25]. Sections were stained using an Anti-CD3 antibody (Abcam, ab5690). An HRP system was used for detection. Positive cells were scanned and counted.

Statistical analyses

GraphPad Prism 6.0 was used for the statistical analysis of data. One-way ANOVA, two-way ANOVA with Bonferroni post-test, or unpaired, two-tailed t-tests were used for as appropriate. Symbols indicate statistical significance as *P < 0.05; **P < 0.01; ***P < 0.001. Each experiment was performed at least three times.

Discussion

We have described the design, development, and testing of CAR-T cell therapy targeting GPC3 that co-expresses IL-7 and PH20 as a potential treatment for HCC. Compared with G3CAR, G3CAR-7 × 20 has a greater *in vivo* and *in vitro* expansion capacity. Additionally, after activation by tumor cells, G3CAR-7 × 20 demonstrates enhanced expansion and resistance to cell apoptosis. We also observed that G3CAR-7 × 20 is more invasive than G3CAR *in vivo* and *in vitro*, and should infiltrate tumor tissue more effectively *in vivo*.

Few clinical projects have investigated CAR-T therapy of HCC. In a phase I clinical trial targeting GPC3, the overall 1-year survival rate of 13 patients tested was 42%, and the partial response rate was 15.4% (2/13). Compared to CAR-T targeting CD19 for hematological malignancies, CAR-T targeting GPC3 for hepatocellular carcinoma did not show encouraging efficacy[22]. Various factors affect the therapeutic benefit of CAR-T on HCC, such as a poor tumor tissue microenvironment that limits proliferation and CAR-T cytotoxicity and the dense ECM which limits lymphocyte infiltration into tumor tissue[13, 25].

IL-7 is known to have a positive effect on memory phenotype maintenance and CAR-T proliferation during in vitro CAR-T culture[16, 26]. However, addition of IL-7 during *in vitro* culture increases the cost of preparation and is not suitable consistently for clinical applications of CAR-T. Nor can IL-7 added *in vitro* have a long-term effect on CAR-T cells re-infused into the body. Here, we satisfy the *in vivo* and *in vitro* need for IL-7 by co-expressing it with CAR.

To solve the problem of CAR-T's inability to infiltrate tumors effectively, we co-expressed hyaluronidase PH20 (sperm adhesion molecule 1 or SPAM 1) on the CAR-T surface. PH20 is the most active human hyaluronidase[19]. It is involved in fertilization and is expressed in the head and acrosome of human spermatozoa. PH20 is active at pH 5–8, a value similar to that found in the microenvironment of tumor tissue. To maximize safety, hyaluronidase activity should be membrane-linked rather than secreted. PH20 is membrane-bound, anchored on the cell surface by GPI[27]. PH20 has featured in many clinical studies of oncology drugs. For example, the phase 1b PAVO (MMY1004) study evaluated subcutaneous daratumumab targeting CD38 combined with recombinant human PH20 to treat relapsed or refractory MM. Responses of 25.0% and 42.2% were seen when dosed at 1200 mg and 1800 mg[28].

Although PH20 is widely used in clinical trials, our study is the first to seek experimental verification of its function. Keishi Adachi *et al*. have reported that overexpression of IL-7 and CCL19 on CAR-T cells can enhance the proliferation and chemotaxis of CAR-T[26]. We had several reasons for choosing PH20 over

CCL19. First, the editing of large genes is a major limiting factor when modifying T cells, as they increase the difficulty of lentivirus packaging, reduce the ability of lentivirus to infect cells, and thus increase the cost of the procedure[29, 30]. Secondly, GPC3 is reported to be a very specific target, and thus CAR-T targeting of it is thought not to have off-target toxicity[22, 31, 32]. Therefore, we believe that for CAR-T targeting GPC3 or other specific solid tumor targets, increasing CAR-T's infiltration ability is better than increasing its capacity for chemotaxis. CAR-T cells infiltrating tumor tissue are restricted by the tumor microenvironment, preventing it from exerting its full tumor-killing function. In principle, IL-7 expressed simultaneously with PH20 can effectively regulate the tumor tissue microenvironment, allowing CAR-T to function optimally.

Conclusion

In conclusion, we have for the first time described CAR-T cells that target GPC3 while co-expressing IL-7 and PH20 as a potential treatment for HCC, suggesting that it, and the strategy it embodies, may in time become a promising and powerful future clinic treatment in oncology.

Declarations

Acknowledgment

This work was supported by the Guangxi clinic medicine research center of hepatobiliary diseases (AD17129025).

Conflict of interest

The authors declare that there is no conflict of interest.

Data Availability Statement

The data used to support the findings of this study are available from the corresponding author upon request.

Author contributions

Su-yang Yue designed the study and collected the data and made the analysis. Qian Liu, Cixiao Wang and Zeyou Jiang performed the experiments. All of the authors approved the final proof.

Ethics approval and consent to participate

This study was approved by the Ethics Committee of the Xuzhou Medical University

References

1. Alcantara M, Tesio M, June CH, Houot R. CAR T-cells for T-cell malignancies: challenges in distinguishing between therapeutic, normal, and neoplastic T-cells. Leukemia 2018; 32: 2307-2315.
2. Chavez JC, Locke FL. CAR T cell therapy for B-cell lymphomas. Best Pract Res Clin Haematol 2018; 31: 135-146.
3. Vitale C, Strati P. CAR T-Cell Therapy for B-Cell non-Hodgkin Lymphoma and Chronic Lymphocytic Leukemia: Clinical Trials and Real-World Experiences. Front Oncol 2020; 10: 849.
4. Zhang J, Li J, Ma Q et al. A Review of Two Regulatory Approved Anti-CD19 CAR T-Cell Therapies in Diffuse Large B-Cell Lymphoma: Why Are Indirect Treatment Comparisons Not Feasible? Adv Ther 2020; 37: 3040-3058.
5. D'Agostino M, Raje N. Anti-BCMA CAR T-cell therapy in multiple myeloma: can we do better? Leukemia 2020; 34: 21-34.
6. Raje N, Berdeja J, Lin Y et al. Anti-BCMA CAR T-Cell Therapy bb2121 in Relapsed or Refractory Multiple Myeloma. N Engl J Med 2019; 380: 1726-1737.
7. Zhao WH, Liu J, Wang BY et al. A phase 1, open-label study of LCAR-B38M, a chimeric antigen receptor T cell therapy directed against B cell maturation antigen, in patients with relapsed or refractory multiple myeloma. J Hematol Oncol 2018; 11: 141.
8. Hege KM, Bergsland EK, Fisher GA et al. Safety, tumor trafficking and immunogenicity of chimeric antigen receptor (CAR)-T cells specific for TAG-72 in colorectal cancer. J Immunother Cancer 2017; 5: 22.
9. Tchou J, Zhao Y, Levine BL et al. Safety and Efficacy of Intratumoral Injections of Chimeric Antigen Receptor (CAR) T Cells in Metastatic Breast Cancer. Cancer Immunol Res 2017; 5: 1152-1161.
10. Zhang C, Wang Z, Yang Z et al. Phase I Escalating-Dose Trial of CAR-T Therapy Targeting CEA(+) Metastatic Colorectal Cancers. Mol Ther 2017; 25: 1248-1258.
11. Habib R, Nagrial A, Micklethwaite K, Gowrishankar K. Chimeric Antigen Receptors for the Tumour Microenvironment. Adv Exp Med Biol 2020; 1263: 117-143.
12. Rodriguez-Garcia A, Palazon A, Noguera-Ortega E et al. CAR-T Cells Hit the Tumor Microenvironment: Strategies to Overcome Tumor Escape. Front Immunol 2020; 11: 1109.
13. Owyong M, Efe G, Owyong M et al. Overcoming Barriers of Age to Enhance Efficacy of Cancer Immunotherapy: The Clout of the Extracellular Matrix. Front Cell Dev Biol 2018; 6: 19.
14. Donnadieu E, Dupre L, Pinho LG, Cotta-de-Almeida V. Surmounting the obstacles that impede effective CAR T cell trafficking to solid tumors. J Leukoc Biol 2020.
15. Arcangeli S, Falcone L, Camisa B et al. Next-Generation Manufacturing Protocols Enriching TSCM CAR T Cells Can Overcome Disease-Specific T Cell Defects in Cancer Patients. Front Immunol 2020; 11: 1217.

16. Zhou J, Jin L, Wang F et al. Chimeric antigen receptor T (CAR-T) cells expanded with IL-7/IL-15 mediate superior antitumor effects. Protein Cell 2019; 10: 764-769.
17. Hong Y, Kim YK, Kim GB et al. Degradation of tumour stromal hyaluronan by small extracellular vesicle-PH20 stimulates CD103(+) dendritic cells and in combination with PD-L1 blockade boosts anti-tumour immunity. J Extracell Vesicles 2019; 8: 1670893.
18. Locke KW, Maneval DC, LaBarre MJ. ENHANZE((R)) drug delivery technology: a novel approach to subcutaneous administration using recombinant human hyaluronidase PH20. Drug Deliv 2019; 26: 98-106.
19. Weber GC, Buhren BA, Schrumpf H et al. Clinical Applications of Hyaluronidase. Adv Exp Med Biol 2019; 1148: 255-277.
20. Chaudhari VA, Khobragade K, Bhandare M, Shrikhande SV. Management of fibrolamellar hepatocellular carcinoma. Chin Clin Oncol 2018; 7: 51.
21. Sim HW, Knox J. Hepatocellular carcinoma in the era of immunotherapy. Curr Probl Cancer 2018; 42: 40-48.
22. Shi D, Shi Y, Kaseb AO et al. Chimeric Antigen Receptor-Glypican-3 T-Cell Therapy for Advanced Hepatocellular Carcinoma: Results of Phase I Trials. Clin Cancer Res 2020.
23. Kubo N, Araki K, Kuwano H, Shirabe K. Cancer-associated fibroblasts in hepatocellular carcinoma. World J Gastroenterol 2016; 22: 6841-6850.
24. Li W, Guo L, Rathi P et al. Redirecting T Cells to Glypican-3 with 4-1BB Zeta Chimeric Antigen Receptors Results in Th1 Polarization and Potent Antitumor Activity. Hum Gene Ther 2017; 28: 437-448.
25. Caruana I, Savoldo B, Hoyos V et al. Heparanase promotes tumor infiltration and antitumor activity of CAR-redirected T lymphocytes. Nat Med 2015; 21: 524-529.
26. Adachi K, Kano Y, Nagai T et al. IL-7 and CCL19 expression in CAR-T cells improves immune cell infiltration and CAR-T cell survival in the tumor. Nat Biotechnol 2018; 36: 346-351.
27. Fang S, Hays Putnam AM, LaBarre MJ. Kinetic investigation of recombinant human hyaluronidase PH20 on hyaluronic acid. Anal Biochem 2015; 480: 74-81.
28. Usmani SZ, Nahi H, Mateos MV et al. Subcutaneous delivery of daratumumab in relapsed or refractory multiple myeloma. Blood 2019; 134: 668-677.
29. Cai Y, Mikkelsen JG. Lentiviral Delivery of Proteins for Genome Engineering. Curr Gene Ther 2016; 16: 194-206.
30. McCarron A, Donnelley M, McIntyre C, Parsons D. Challenges of up-scaling lentivirus production and processing. J Biotechnol 2016; 240: 23-30.
31. Nishida T, Kataoka H. Glypican 3-Targeted Therapy in Hepatocellular Carcinoma. Cancers (Basel) 2019; 11.
32. Zhou F, Shang W, Yu X, Tian J. Glypican-3: A promising biomarker for hepatocellular carcinoma diagnosis and treatment. Med Res Rev 2018; 38: 741-767.

Figures

Figure 1

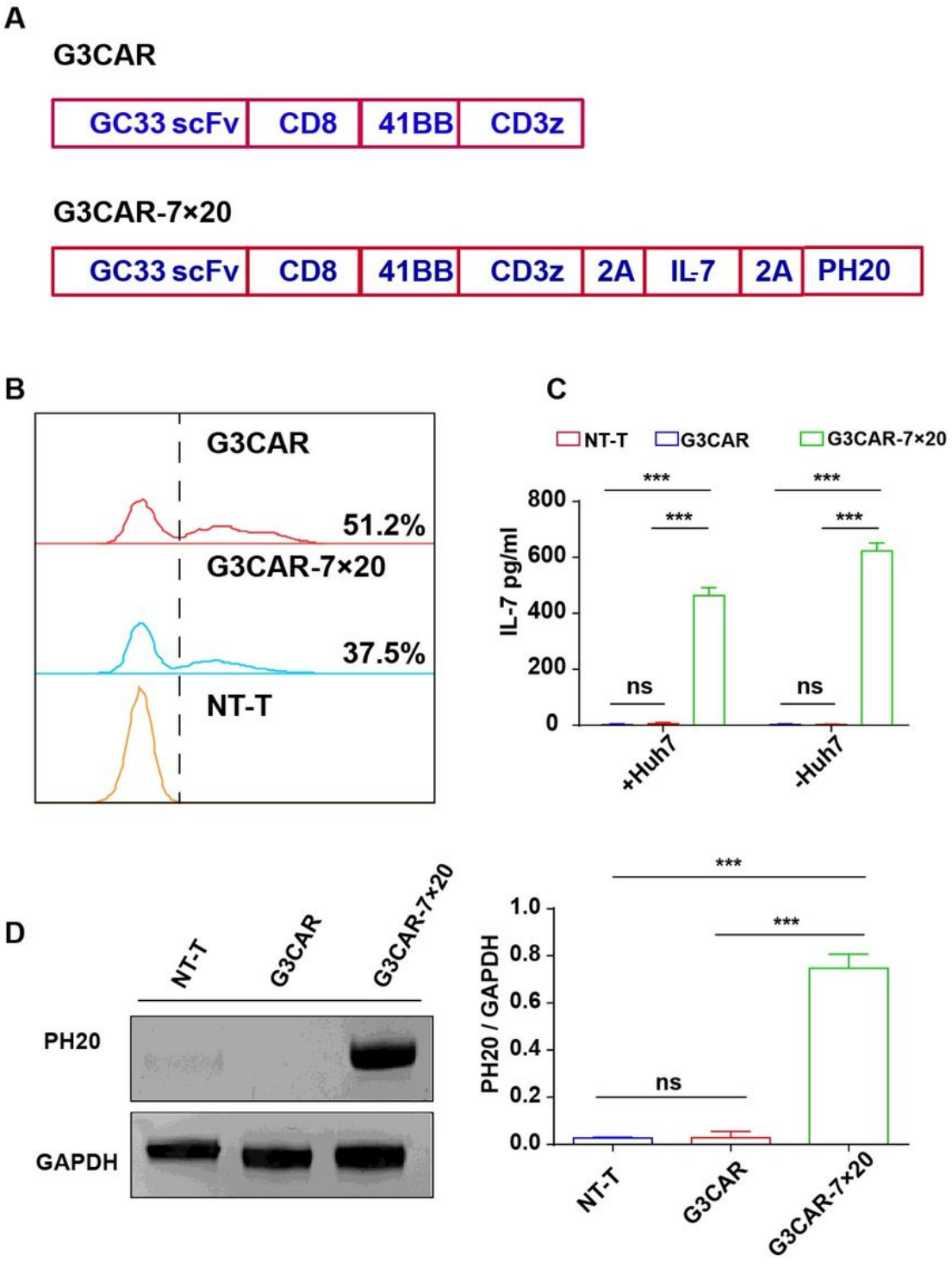

Figure 1

Characterization of CAR-T: A) Schematic diagram of CAR structure; B) Transfection efficiency of CAR-Ts; C) expression of IL-7 in NT-T, G3CAR, and G3CAR-7×20 with or without tumor cell stimulation; D) Expression of PH20 in NT-T, G3CAR, and G3CAR-7×20. Error bars represent mean ± SD (n=3); ***p < 0.001.

Figure 2

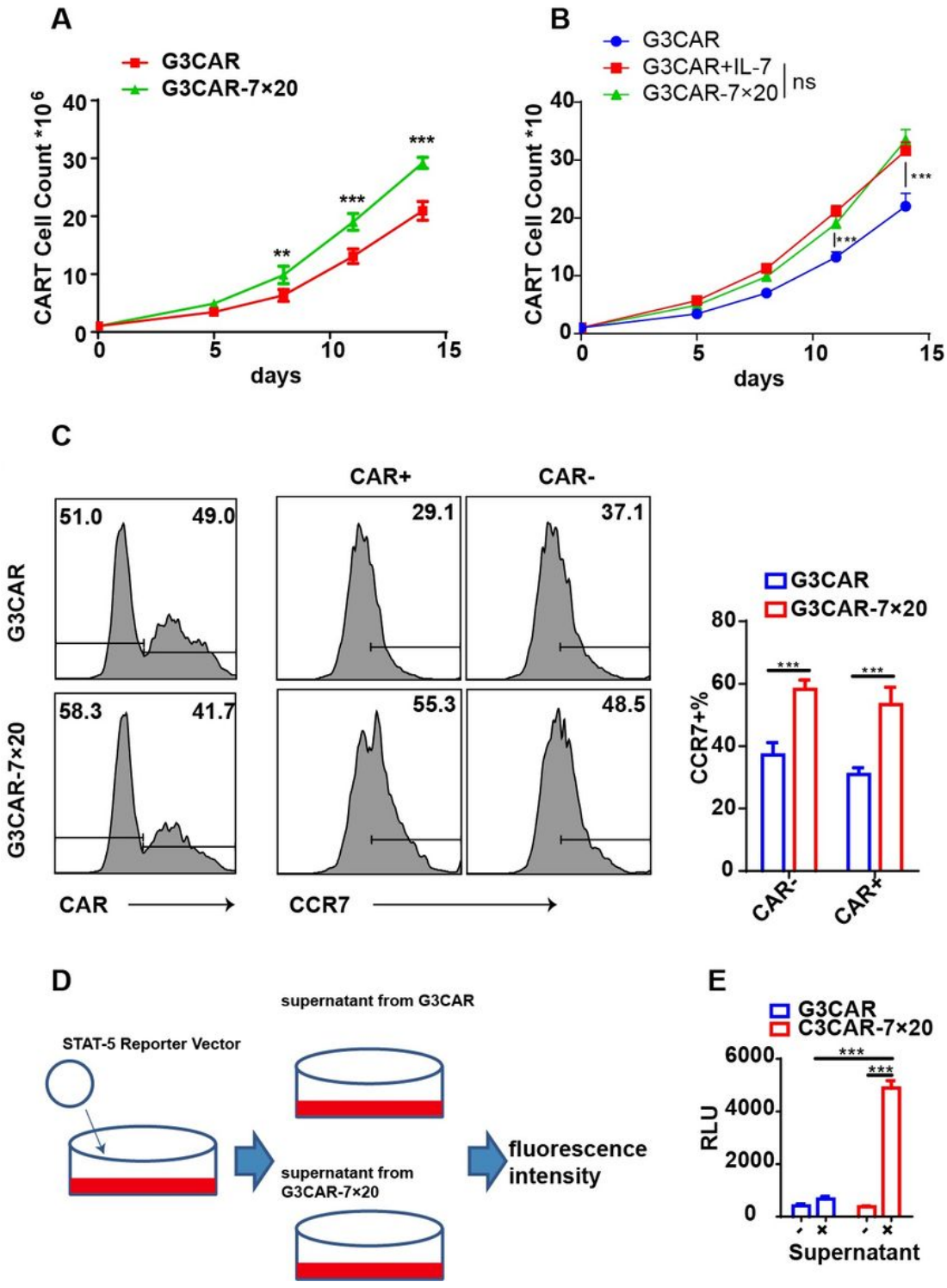

Figure 2

Functional identification of overexpressed IL-7: A) proliferation of G3CAR and G3CAR-7×20; B) G3CAR supplement with additional IL-7; C) memory phenotype of G3CAR and G3CAR-7×20; D) schematic diagram of the STAT5 reporter assay; E) fluorescence intensity measured by STAT5 signal. Error bars represent mean ± SD (n=3); **p < 0.01; ***p<0.001.

Figure 3

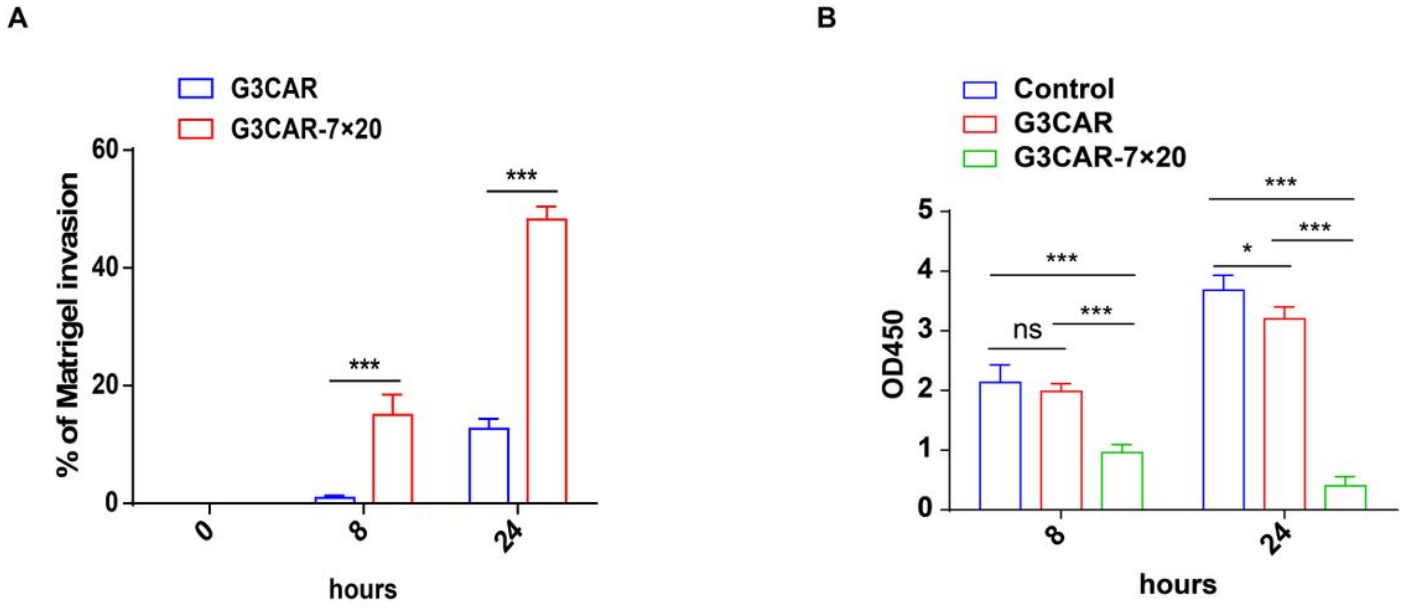

Figure 3

Functional identification of overexpressed PH20: A) identification of G3CAR and G3CAR-7×20 invasion ability in vitro; B) identification PH20 mediated degradation of extracellular matrix. Error bars represent mean ± SD (n=3); ns, no significant difference *p < 0.05; ***p<0.001.

Figure 4

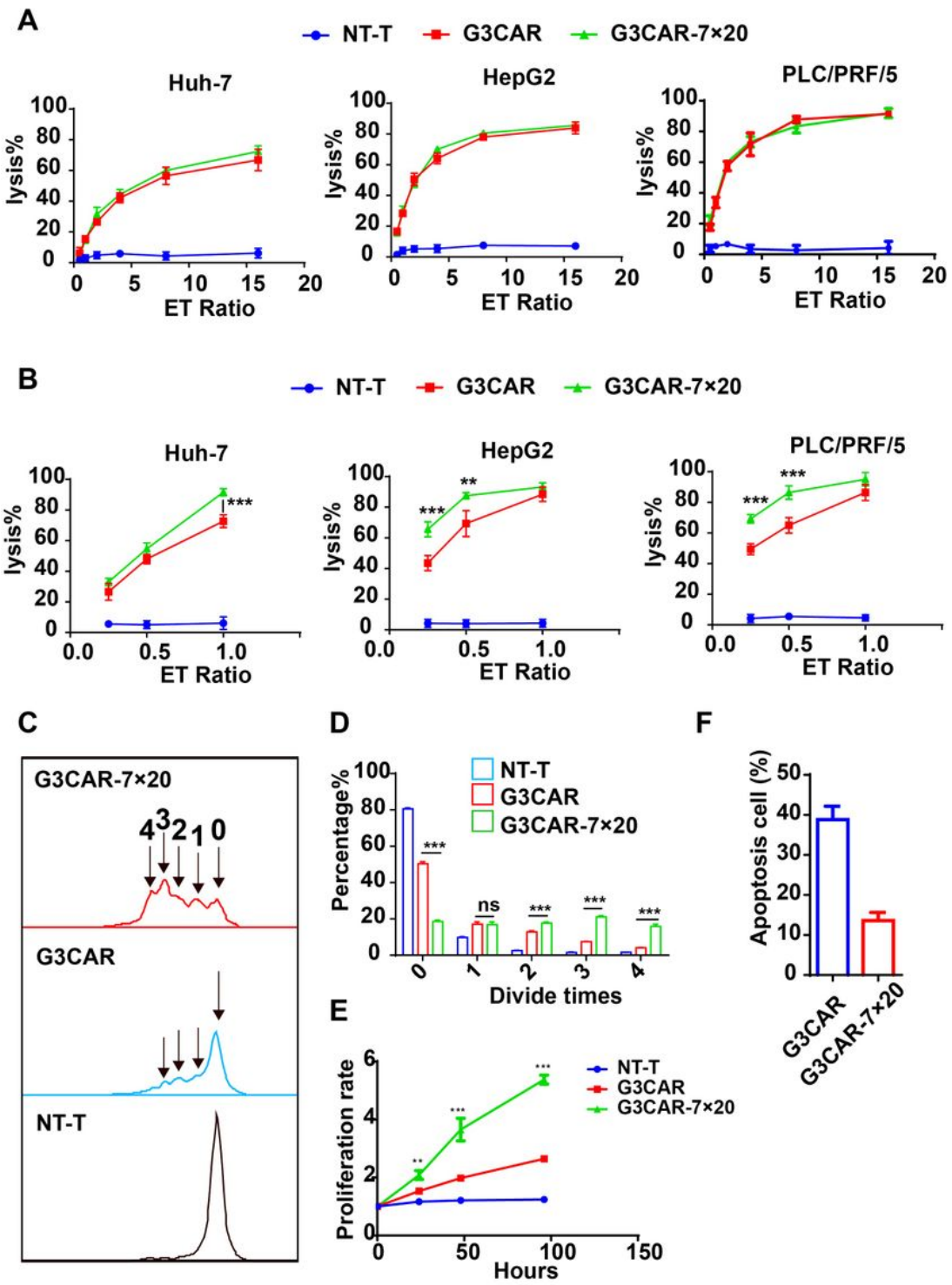

Figure 4

Identification of tumor cell killing activity. Cytotoxicity against tumor cells: short-term (panel A) or long-term (B). Identification of CAR-T division (C) and (D), proliferation (E), and apoptosis (F) after activation by tumor cells. Error bars represent mean ± SD (n=3); ns, no significant difference **p < 0.01; ***p<0.001.

Figure 5

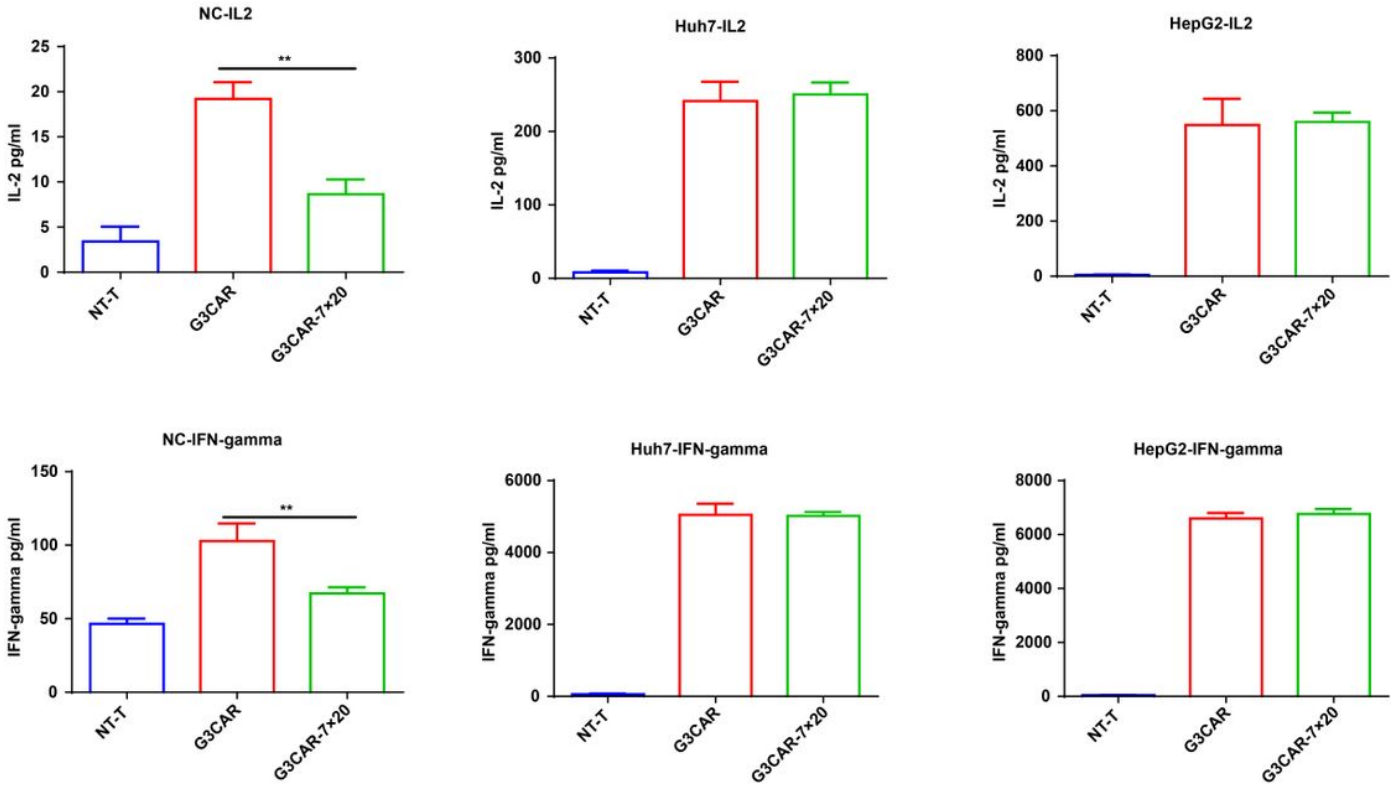

Figure 5

Cytokines secreted after tumor cell encounter. Error bars represent mean± SD (n=3); **p < 0.01.

Figure 6

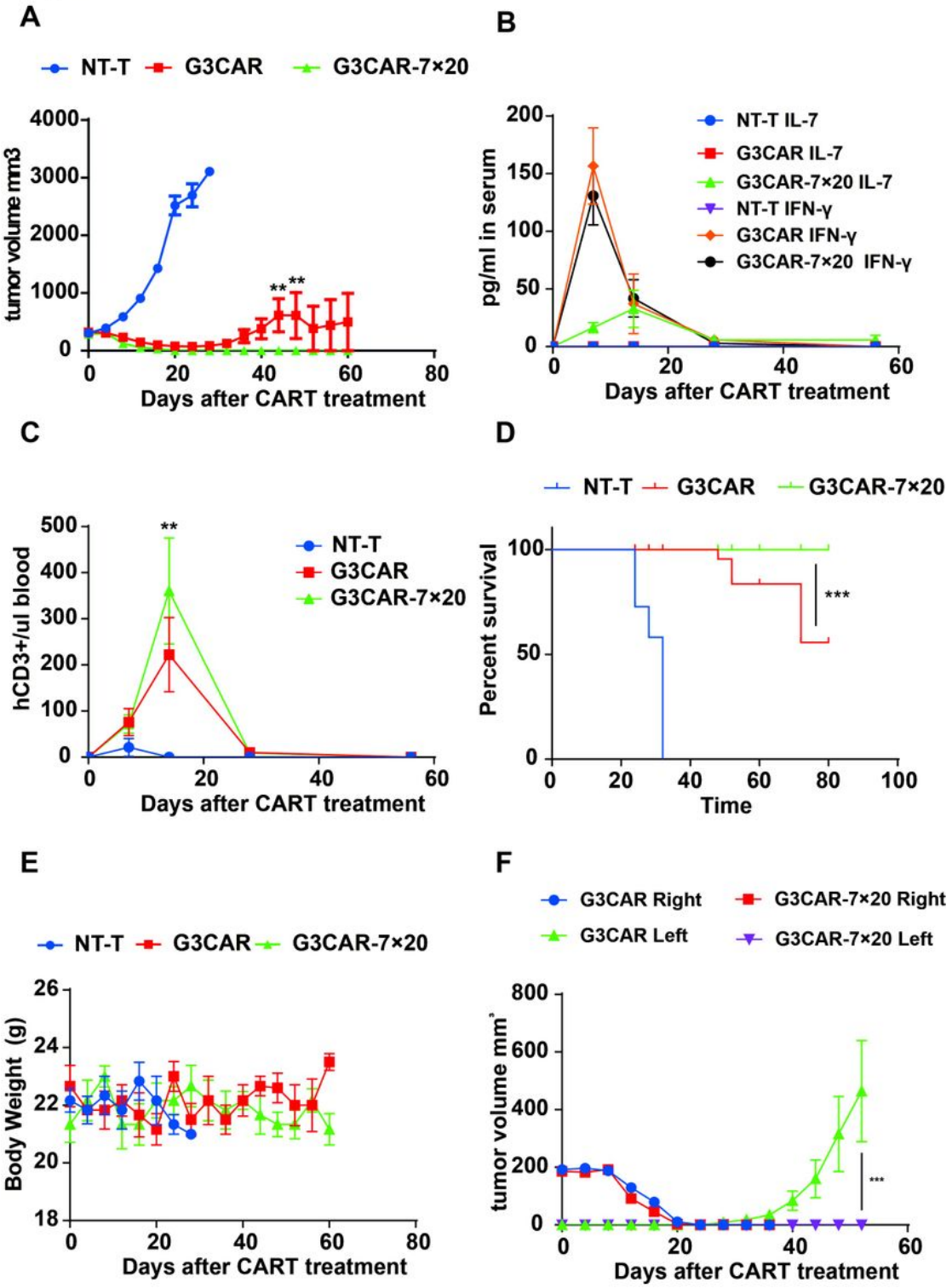

Figure 6

CAR-T cell functional identification in vivo: A) the curve of tumor volume measured using Vernier calipers; B) identification of IL-7 and IFN-gamma levels in serum at five time points (day 0, 7, 14, 28, 56 after CAR-T infusion); C) identification of hCD3 cells in peripheral blood; D) mouse survival presented as Kaplan-Meier curves; E) mouse body weight; F) tumor volume in the re-challenge model. Error bars represent mean ± SEM (n=6); **p<0.01; ***p<0.001.

Figure 7

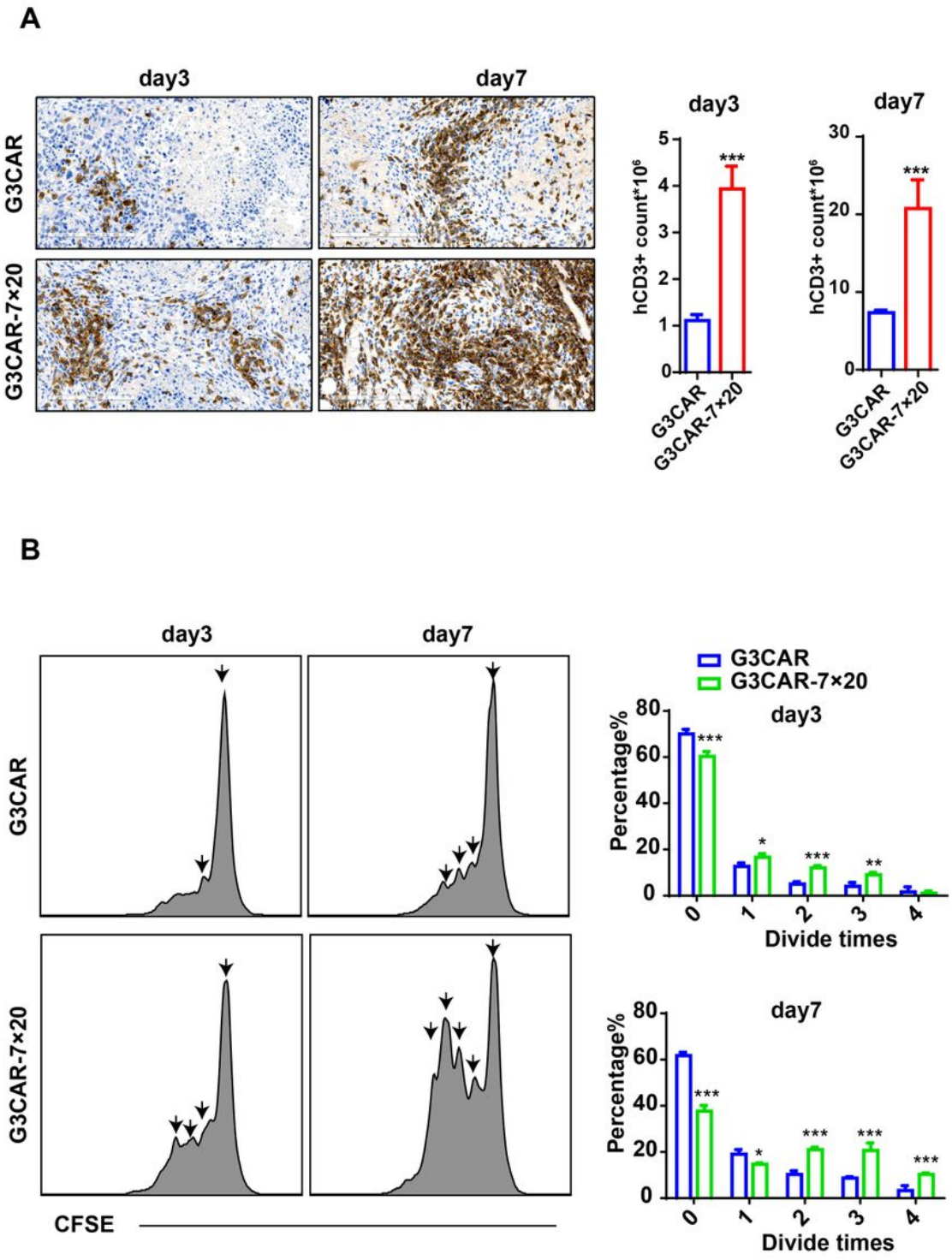

Figure 7

Identification of T cells infiltrating into the tumor: A) histological studies of human CD3 infiltration into tumor tissue at day 3 and day 7 after CAR-T infusion; B) identification of T cell division level after infiltrating into tumor tissue. Error bars represent mean ± SD (n=3); *p<0.05 **p<0.01; ***p<0.001.